Quarry-Induced Slope Instability at a Broadcasting Transmission Plant near Valcava, Lombardia, Italy

***Monica Barbero**, Assistant professor, Politecnico di Torino (Torino, Italy); email: monica.barbero@polito.it*
***Fabrizio Barpi**, Assistant professor, Politecnico di Torino (Torino, Italy); email: fabrizio.barpi@polito.it*

ABSTRACT: *Since 2006, a broadcasting tower and ancillary buildings on the top of a hill adjacent to a large, active limestone quarry, in northern Italy near the village of Valcava, has been heavily damaged by ground deformation due to slope instability. In 2005, the quarry began to work the slope toward the broadcasting plant, releasing bedding planes that affected the tower site: a number of fractures occurred in the warehouse and in the ground around it, that grew particularly during significant rainfalls. In October 2006 a landslide occurred in the quarry area, close to the broadcasting site. In order to understand what induced the fracture process in the buildings and define a support system to stabilize the broadcasting site, a detailed geotechnical survey and a number of numerical slope stability analyses were carried out. One of the main goals of the paper is to underline the effectiveness of the numerical analyses to understand the instability phenomena when they are particularly complex. Furthermore, by using a reliable numerical model with a good understanding of site geology and of the main geotechnical parameters, an evaluation of the slope behavior under different scenarios was made and stabilization measures can be designed.*

KEYWORDS: damage, landslide, slope instability, stabilization system, numerical analysis.

SITE LOCATION: IJGCH-database.kmz (requires Google Earth)

INTRODUCTION

The broadcasting tower and ancillary buildings are located at 45°47′N, 9°31′E on the top of a hill, 1390 m above sea level, in Northern Italy (Lombardia region, close to the village of Valcava). The geological map of the site is presented in Figure 1. The most damaged building is a warehouse where many sensitive electronic instruments are installed, is very close to the edge of the slope. At the time of the plant construction, a quarry was operating on the hillside, but operations were restricted away from the tower site.

In 2005, quarry operations initiated at the slope toward the broadcasting tower. In May 2006, tension cracks developed in the ground at the top of the hill and many cracks appeared in the walls and floor of the building (Figures 2 and 3). The cracks were parallel to the slope face, suggesting a downward movement of the slope. In October 2006, after two days of medium-high intensity rains, a landslide with a volume of about 27000 m^3 occurred in the pit (Figure 4 and 5) at a distance of about 45 m below the warehouse area (Figure 6) and the cracks in the warehouse and in the ground increased, the latter reaching openings of some centimeters. The intense rains of the winter 2006 quickened instability phenomena (Barbero et al., 2008).

In 2007, the authors were asked to study the problem to identify the main causes of instability and suggest an adequate stabilization system to ensure the safety of the plant. For this purpose, geological and geotechnical surveys were undertaken and numerical analyses were performed. These are detailed below.

Submitted: 21 April 2011; Published: 16 November 2011
Reference: Barbero, M., Barpi, F. (2011). *Quarry-Induced Slope Instability at a Broadcasting Transmission Plant Near Valcava, Lombardia, Italy.* International Journal of Geoengineering Case histories, http://casehistories.geoengineer.org, Vol.2, Issue 2, p.163-181. doi: 10.4417/IJGCH-02-02-04

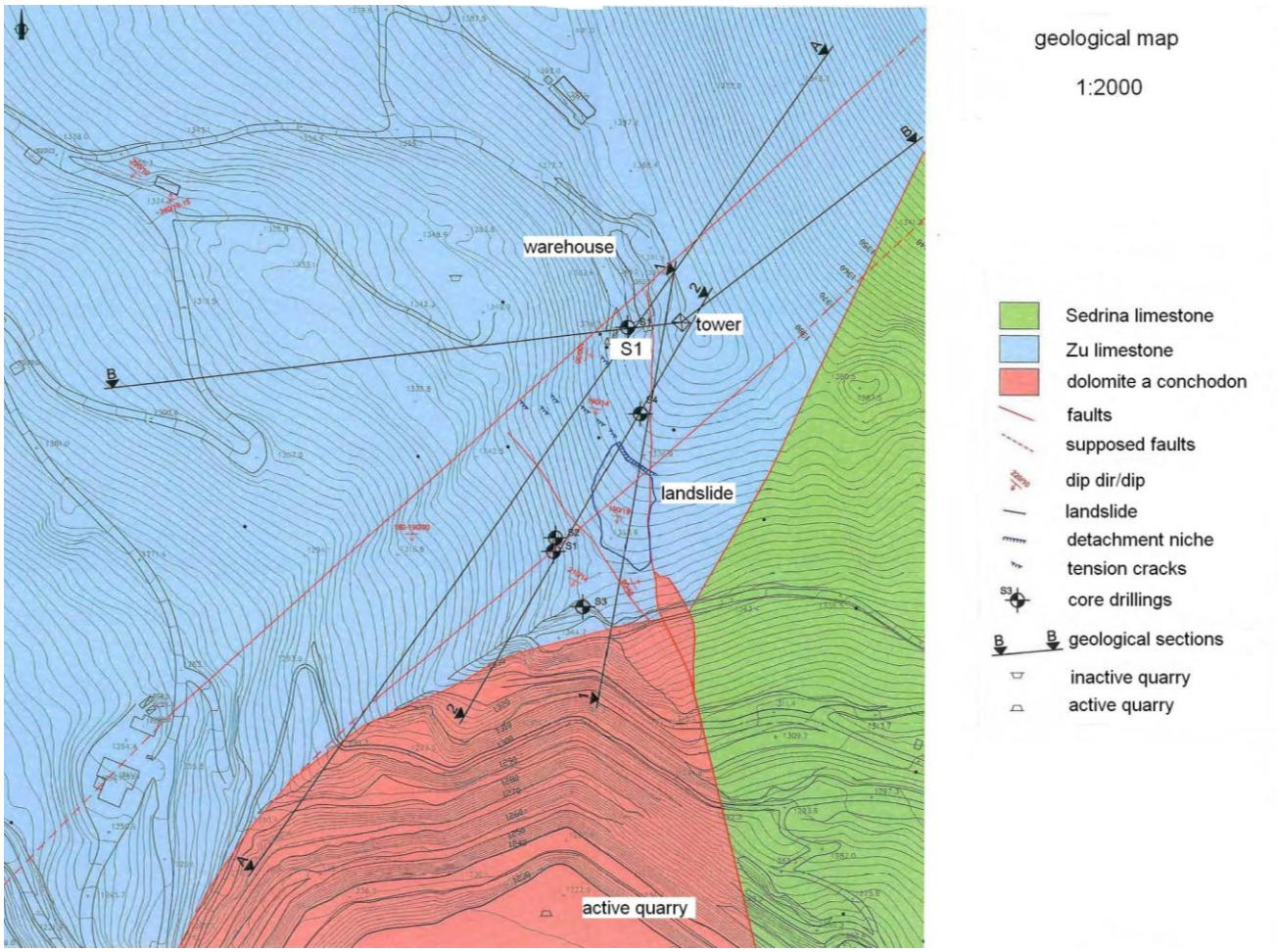

Figure 1. Geological map of the site.

FIELD INVESTIGATION AND RESULTS

The first step in analyzing slope instability is the geotechnical and geological characterization of the site. For this scope, field surveys are best suited. A critical interpretation of the survey results allow the development of a model to simulate the instability phenomenon, with the aim to ascertain the main causes that induced it. The same model can then be used for the verification of the predicted stabilization system.

In this case study, detailed geological and geotechnical surveys have been carried out consisting of:

1. geological structural survey,
2. geomorphological survey,
3. core drilling, and installation of inclinometer,
4. seismic refraction surveys of the broadcasting tower site,
5. resistivity outlines close to the seismic ones.

The results obtained are summarized in the following Sections.

Figure 2. Wall damage inside the warehouse.

Figure 3. Floor damage inside the warehouse.

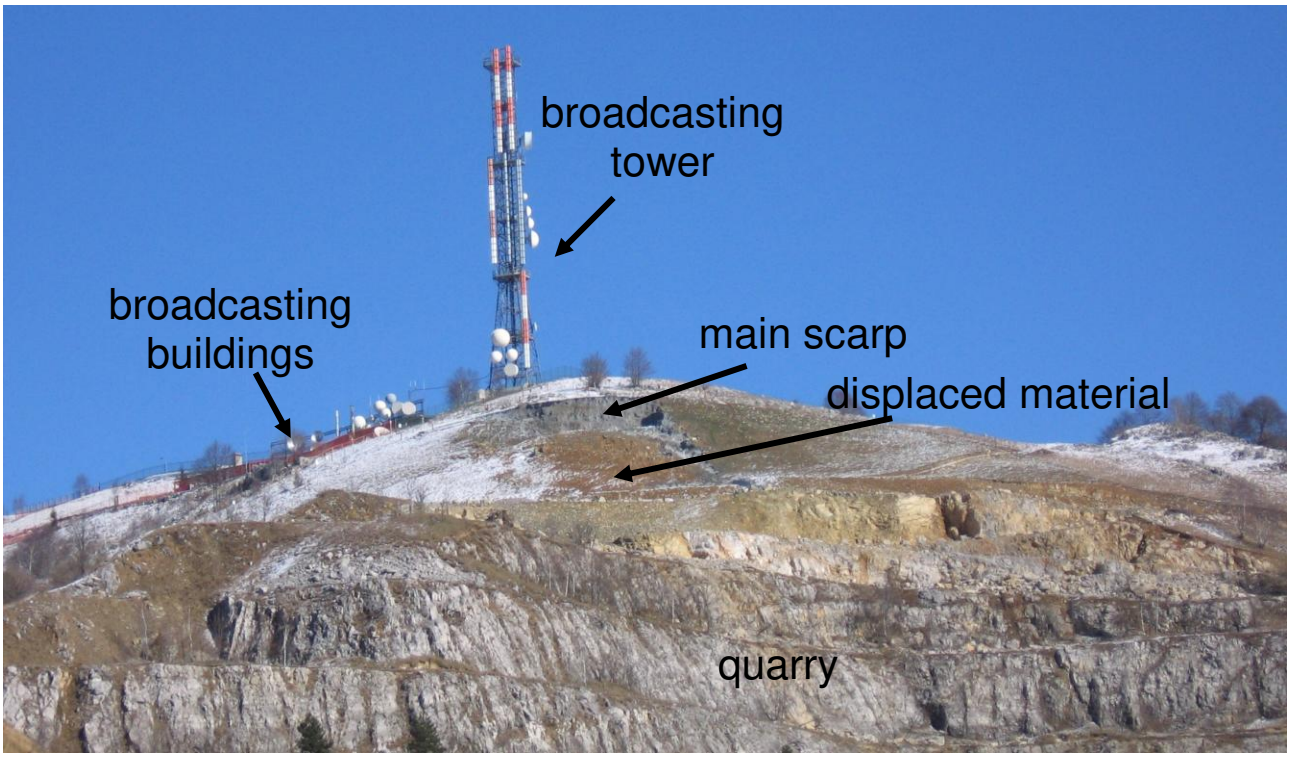

Figure 4. The landslide in the pit area.

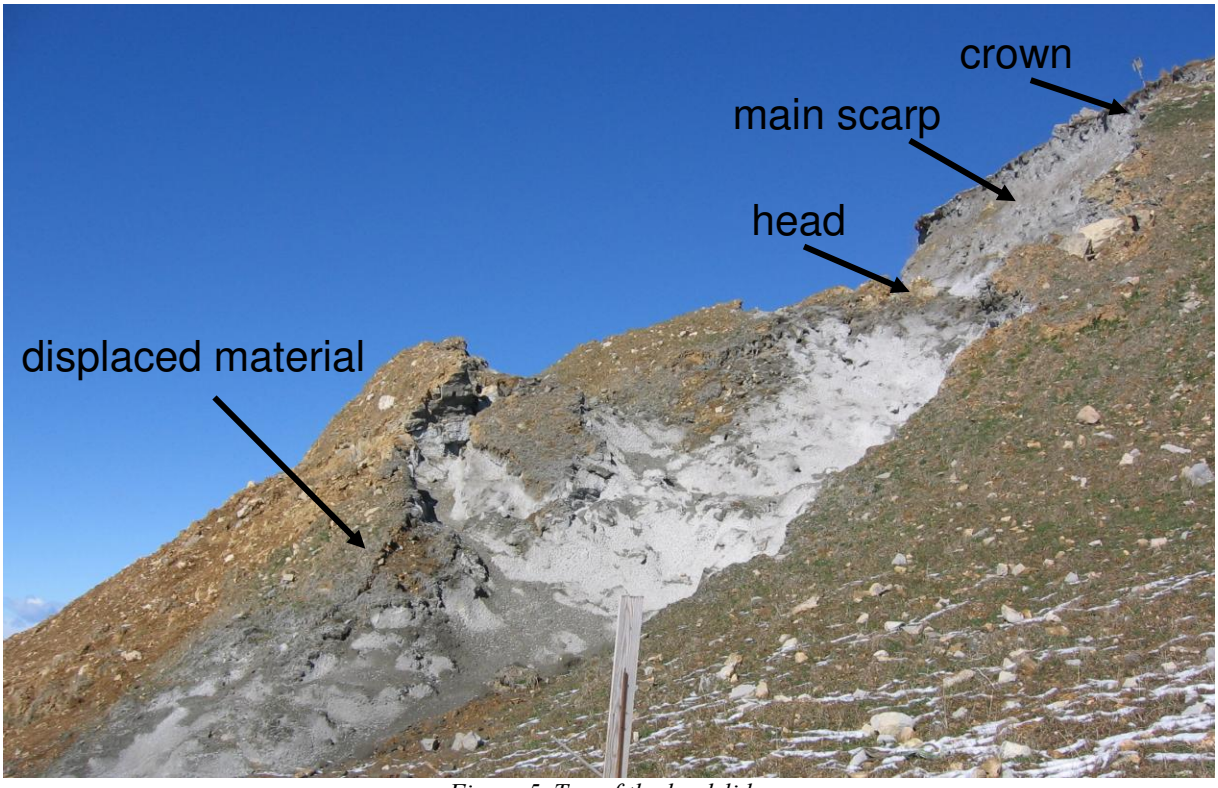

Figure 5. Top of the landslide.

Geological field inspection

The analysis of the geological map (Figure 1) and the results of the geological survey concluded that:

1. Two limestone facies characterized the slope: the Zu limestone and the Sedrina limestone. The geological boundary has tectonic origin and is represented by fault B, in Figure 6. The landslide occurred in the Zu limestone facies, where the presence of marly and argillitic layers facilitated the sliding along the bedding planes;
2. A second fault is present in the slope area (fault A in Figure 6) which intersects the fault B causing strong cataclasis in both facies, with a remarkable reduction of the rock mass quality;
3. Fault A marks the eastern boundary of the landslide in the pit area. This involves a 30 m slope height and has a crown length of about 35 m;
4. In the west side of the edge and in the toe of the landslide, many opened cracks were observed, suggesting that the instability phenomenon is not completed yet and potential landslide progression toward the plant is possible;
5. After the event, the landslide was entirely covered by a layer of sprayed-on concrete. In the edge of the landslide, many tension cracks developed with openings of a few centimeters in width. These confirmed that the slope is still moving.

Geological-geostructural survey

The geological-geostructural survey was performed in three structural stations (shown in Figure 6). Four main discontinuities sets were found to characterize the rock mass (stereographic projections in Figure 6): 10°-15° down slope dipping bedding planes, two sub-vertical sets that can be potential tension cracks and a set parallel to fault B.

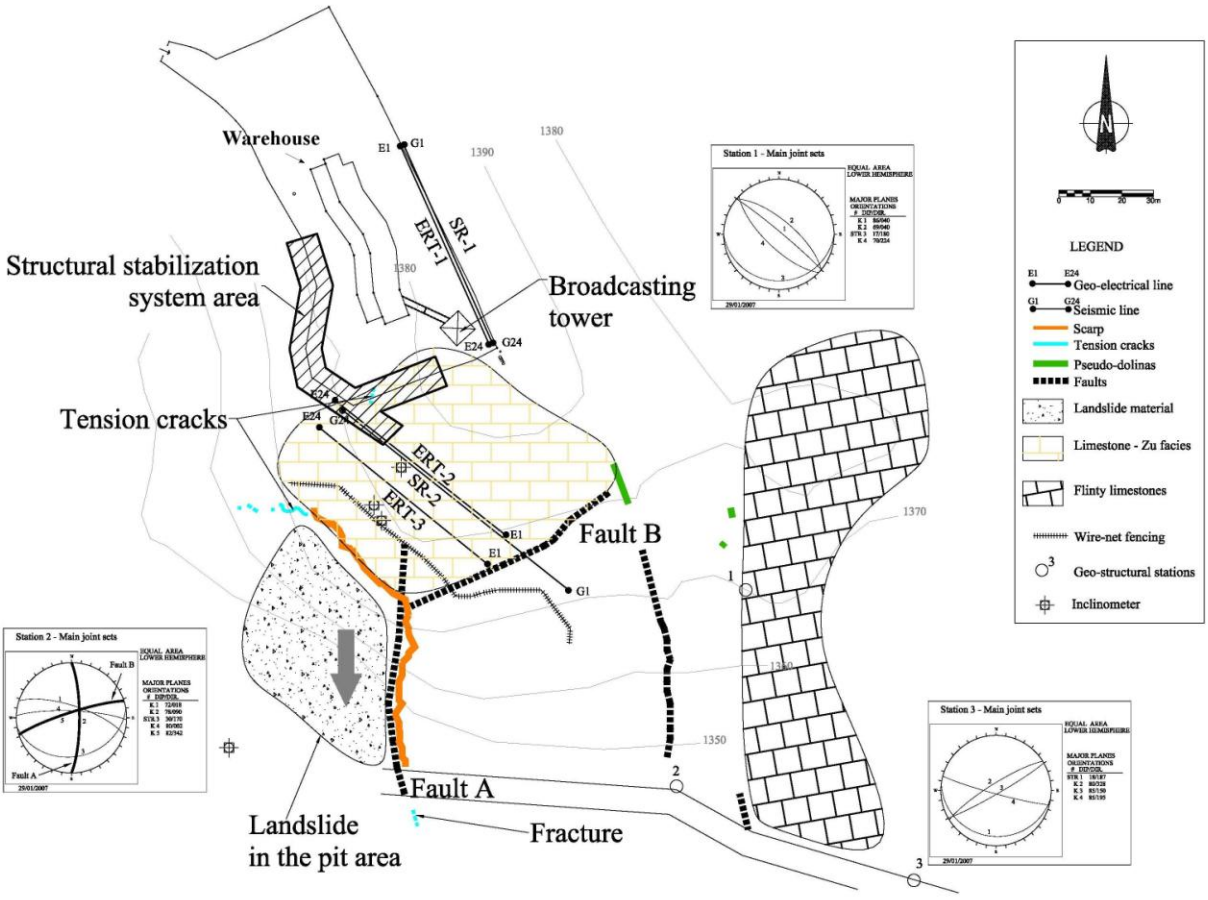

Figure 6. Map of the unstable area and results of the geotechnical survey.

Core drilling

A drill core was taken from a 45 m deep hole drilled adjacent to the building (labeled S1 in Figure 1), near the top of the slope (about 1392 m asl). The core drilling analysis allowed to define the rock mass stratigraphy. Four main geological levels were observed, from the plane of the site: a 3 m thick layer of filling material, about 11 m thick eluvium-colluvial sheet, highly fractured limestone until the depth of about 20 m and limestone bedrock. In situ observation of the main scarp depth suggested that the movement occurred at a depth of about 16 m. Comparing these data it was possible to assert that the contact between the 20 m deep weaker layer and the undamaged bedrock is a preferential sliding zone. At the depth of about 20 m, a cavity with air inside was found, indicating the absence of water bed above the depth of 20 m.
The hole was then instrumented with an inclinometer. The first measurements showed a maximum horizontal displacement gradient of about 6 mm between 8 m and 16 m from the site level in a period of about two months. This movement was confirmed by the opening of the tension cracks occurred in the ground since the installation of the inclinometer.
These results, together with the observation that neither the tower or the other buildings located nearby at the top of the hill showed any damage, suggested that the instability phenomenon was a sliding along the bedding planes, located strictly in the zone between two main faults (A and B, shown in Figures 6 and 7) that intersect close to the warehouse foundations and induce a high damage in the rock mass.

Seismic refraction and geo-electrical survey

One seismic refraction and two geo-electrical soundings were located near the warehouse on the unstable slope, toward the pit. Another pair of seismic and geo-electrical outlines was located close to the broadcasting tower base (Figures 6 and 7).
The data were processed with tomographic technique (Hampson & Russel, 1984; Olsen, 1989) and then interpreted considering the conventional exploration with core-drilling data. Similar results were generated in the slope and in the tower area. Upslope of the warehouse, in the tower area, there is a superficial layer of fill about 3 m deep, underlain by a layer of fractured limestone overlying apparently intact bedrock at a depth of about 16 m, as shown in Figure 8. Near the warehouse, upslope from the landslide, a pit showed the same stratigraphic sequence is observed in the tower area, as well as evidence of the two main faults A and B (Figure 9). Because of fault B, the apparently intact limestone is found at a depth of more than 20 m. The seismic survey thus confirmed the likelihood that the sliding surface was located above a depth of 20 m.

Monitoring structural damage in the warehouse

As crack opening and spreading are important signs of the instability evolution, crack gauges were placed across the larger cracks observed in the warehouse and a continuous monitoring of lengths and openings was performed. Unfortunately, no measurements are available for the cracks that appeared outside the warehouse (tension cracks in Figure 6). The cracks in the warehouse appeared to become more frequent toward the slope in the landslide direction, suggesting that the down slope movement of the rock mass affects the foundation of the warehouse.

Observations

The results of the field surveys have shown that many natural weakness elements affect the site. Fault A marks the east boundary of the landslide. Its intersection with fault B (Figures 6 and 7) induces heavy fracturing in the limestone to significant depths contributing to the instability of the area. The downslope dipping bedding planes predispose the slope to sliding and the two sub-vertical sets of discontinuities can become preferential paths for water percolation.
These favorable to sliding conditions, however, do not result in movement of the instable mass, as no cracks or damage occurred in the broadcasting plant before the pit activities initiated towards the plant. Quarrying activities caused relaxation of the rock along the bedding planes in the excavation area, progressively inducing the landslide. The instability involved also the broadcasting area inducing tension cracks and fractures in the soil and in the warehouse. The tension cracks became preferential paths for the water, so the stability of the area got worse with heavy rainfalls during the spring and the autumn 2006 until the collapse in October 2006. This event mobilized the slope slide in the broadcasting site and the growth of the fractures openings was observed.
However, quarrying activities did not damage the buildings located in the broadcasting site neighbourhood and the broadcasting tower did not exhibit any displacements or rotations. In fact, no changes in the broadcasting signal occurred in that period. These facts allowed ruling out that the landslide was induced by a larger, deep–seated, landslide.

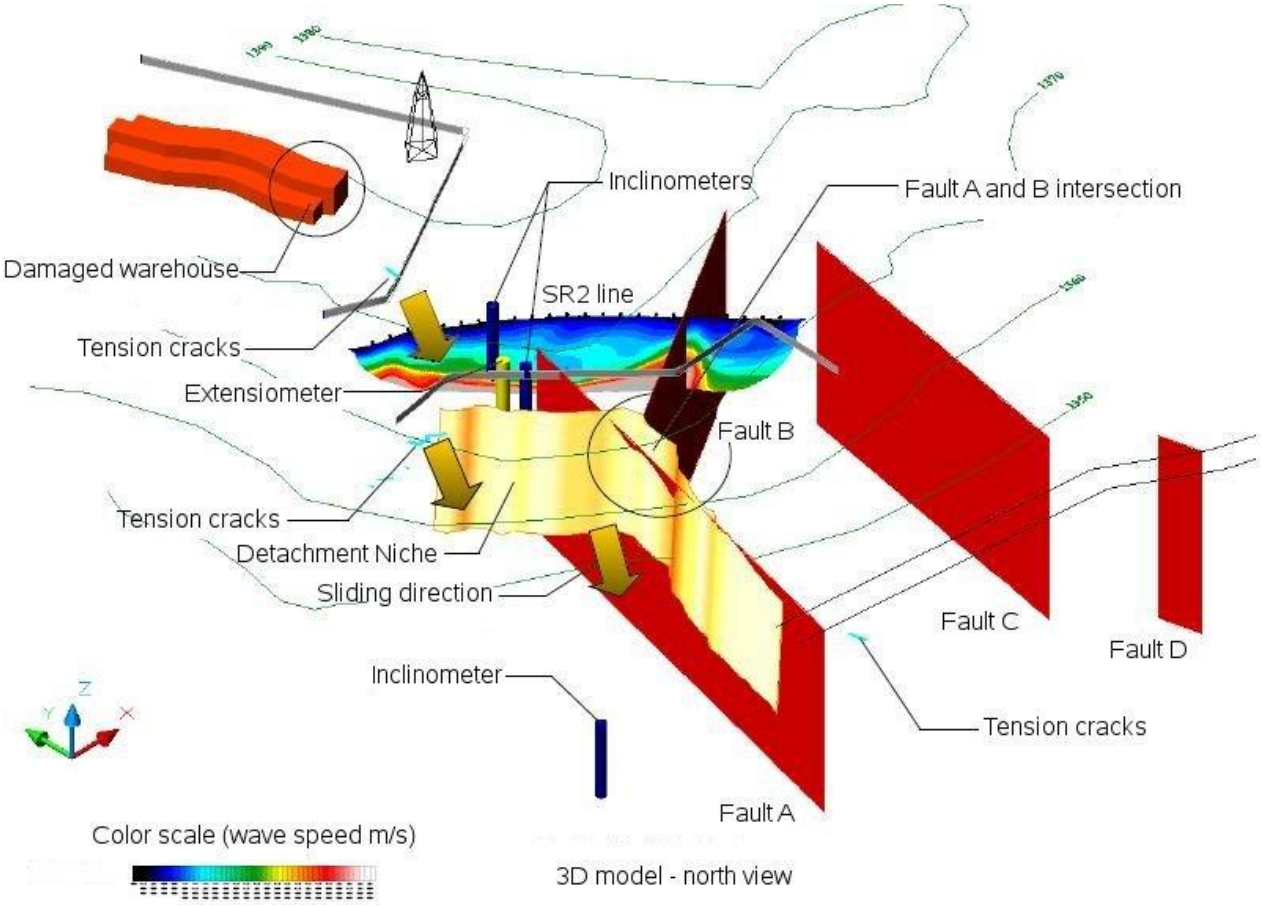

Figure 7. Three dimensional model for the seismic and geo-electrical survey.

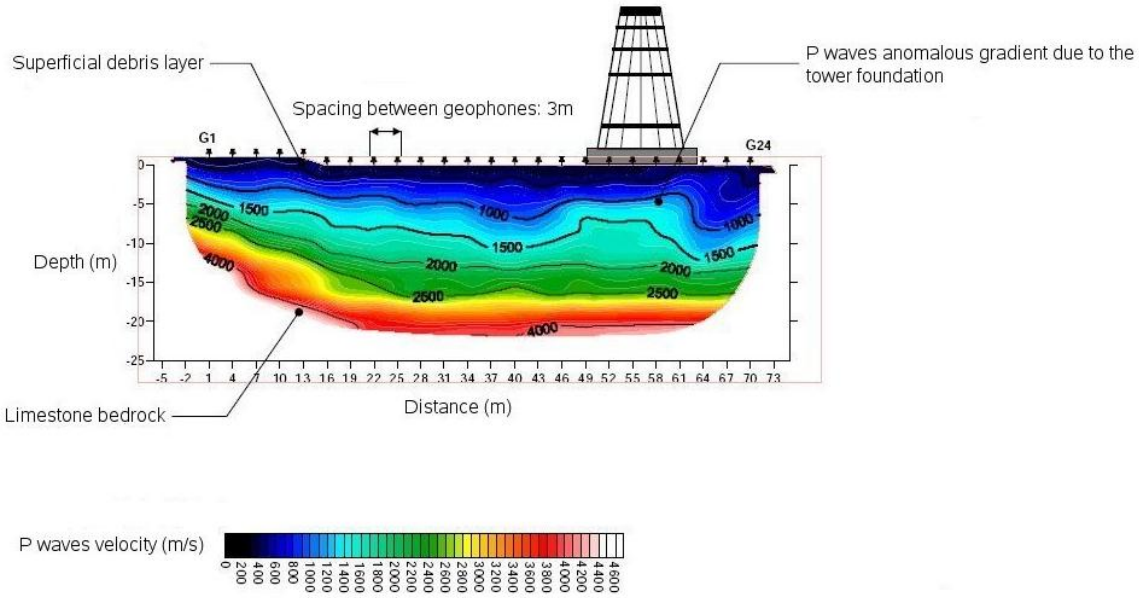

Figure 8. Seismic refraction survey results: P waves velocity trend inside the rock mass near the broadcasting tower.

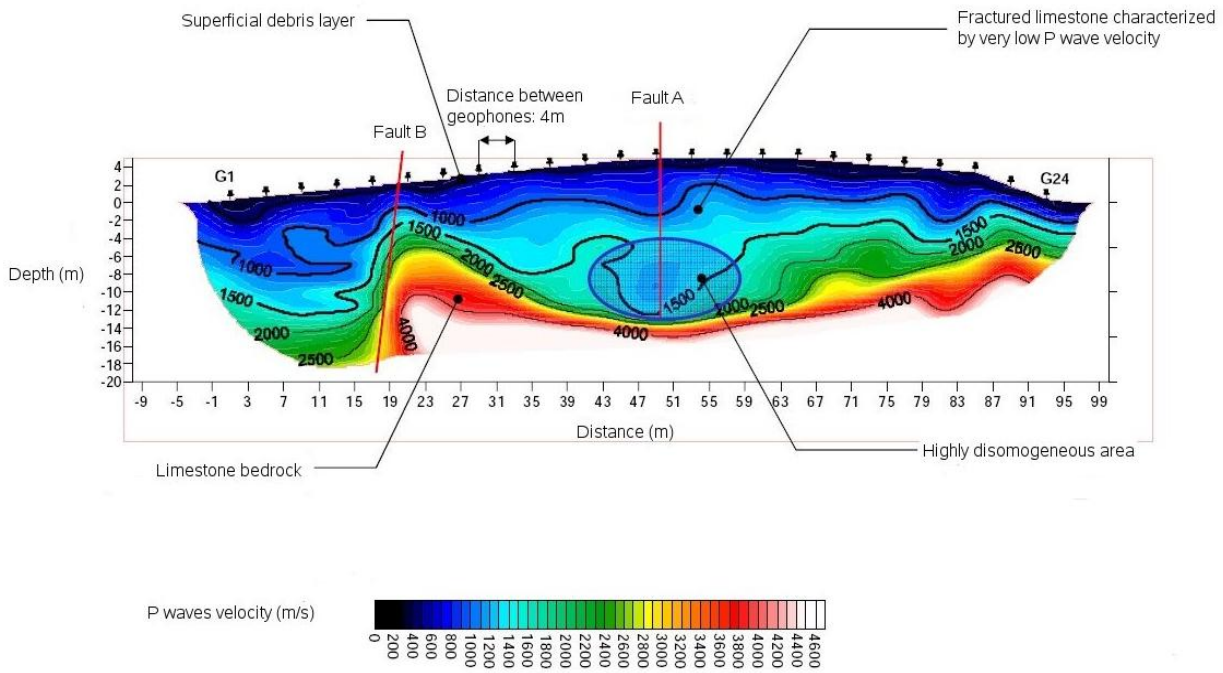

Figure 9. Seismic refraction survey results: P waves velocity trend inside the rock mass, below the warehouse area.

SLOPE STABILITY NUMERICAL ANALYSES

In order to confirm the triggering causes of the slope instability as identified by the field survey results and to suggest an adequate stabilization system to ensure the safety of the plant, a number of numerical simulations were carried out.
On the basis of the results obtained from the field surveys, the slope was modeled as an homogeneous anisotropic equivalent continuum, with the Finite Difference Method (Eberhardt, 2003). First, the original and after the landslide geometry of the slope was considered to confirm the hypothesized instability mechanisms suggested by the field survey. Then, to predict the slope behavior in the state after quarrying activities, further analyses were carried on simulating the operations in the pit (Pelizza et al., 2000; Ferrero et al., 2011). No seismic analyses were carried out because, in compliance with 2007 italian Regulations, the studied area was classified as low seismicity ("zone 4") and in that case no seismic verification was required.

Geotechnical characterization of the rock mass and parameters assessment

The geotechnical classification of the rock mass was performed using the GSI classification index (Hoek et al., 1997). The GSI index was estimated according to the geotechnical survey results. Two geotechnical units were recognized: undisturbed rock mass characterized by a mean GSI of 55 (minimum value equal to 40), and rock mass in the fault zones, with a GSI of 25 (minimum value equal to 10). As no experimental data were available, the rock-mass Hoek and Brown strength parameters (Hoek & Brown, 1980; Hoek et al., 2002) were calculated using intact rock characteristics for limestone experimentally measured in neighboring sites and on limestone samples from the same geological formation: $m_i = 30$, σ_{ci}= 40 MPa (mean value of the uniaxial compressive tests results) for the undisturbed rock mass and σ_{ci}= 13.3 MPa (minimum value of the uniaxial compressive test results) for the disturbed (fault zones). A damage index $D = 0$ was assumed for the rock mass and $D = 0.7$ for the rock mass disturbed by blasting, close to the quarry area. From these data, the parameters collected in Table 1 were calculated for the geotechnical units.

Table 1. Mechanical parameters for the geotechnical units.

Geotechnical unit	Quality conditions	GSI	σ_{ci} (MPa)	m_i (-)	m_b (-)	s_b (-)	σ_{cm} (MPa)	σ_{tm} (MPa)	c (kPa)	φ (°)	γ (kN/m^3)
Undisturbed rock mass	mean	55	40	30	6.01	0.067	3.22	-0.045	436	63	25
	minimum	40			3.52	0.0013	1.32	-0.014	297	60	
Disturbed rock mass	mean	25	13.3	30	2.06	0.0002	0.16	-0.002	142	48	24
	minimum	10			1.206	4.54×10^{-5}	0.04	-0.001	85	42	

Parameters m_b and s_b are the Hoek and Brown criterion parameters for the rock mass, σ_{cm} uniaxial compressive strength for the rock mass, σ_{tm} uniaxial tensile strength for the rock mass, c cohesion (Mohr-Coulomb criterion), φ friction angle (Mohr-Coulomb criterion) and γ rock mass unit weight.

The strain modulus for the rock mass was empirically calculated on the basis of the GSI values (Hoek & Diederichs, 2006). Using deformation moduli for the intact rock ($E_i = MR \cdot \sigma_{ci}$) of 28 GPa and 9.3 GPa for undisturbed and disturbed rock mass, respectively, deformation moduli from 1600 MPa to 11400 MPa and from 300 MPa to 600 MPa were assigned to the undisturbed and disturbed rock masses, respectively.

The mechanical characteristics of the discontinuities in the rock mass have been obtained according to the geotechnical survey data. According to the Barton-Bandis shear strength criterion (Bandis, 1993), the laboratory-scale joint roughness coefficients JRC_0 was assumed from 4 to 10, the joint compressive strength JCS_0 was set equal to the uniaxial compressive strength of the intact rock. The characteristic lengths of discontinuities were assumed to be 20 m at field scale (L_n) and 0.10 m at laboratory scale (L_0). No waving was considered. The parameters JRC_n and JCS_n assumed for the discontinuities in the undisturbed rock mass and in the fault zone are summarized in Table 2.

Table 2. Mechanical parameters for the discontinuities (undisturbed rock mass and fault zone).

	JRC_0 (-)	JCS_0 (MPa)	L_n/L_0 (-)	JRC_n (-)	JCS_n (MPa)	φ_r (°)
Undisturbed rock mass	7	40	200	3.33	13.15	26
Faults zone	7	13.3	200	3.33	4.37	26

For the residual and colluvial soil sheet and the fill materials, the mechanical parameters of Table 3 were assumed. They were derived from experimental tests performed in previous studies.

Table 3. Mechanical parameters for the residual and colluvial soils and fill.

	φ (°)	Residual cohesion c (kPa)	Peak cohesion c_p (kPa)	γ (kN/m^3)
Residual and colluvial soils	From 30° to 33°	0	From 10 to 20	20
Fill	30°	0	-	20

An assumption had to be made for the discontinuity parameters, for which no experimental measurement was available. In order to confirm the suitability of the geotechnical characterization, a back-analysis of the landslide which occurred in October 2006 in the pit area was carried out, using the limit equilibrium method (LEM). The landslide involved an area of about 1750 m^2, between 1345 and 1375 m over sea level. It was assumed that the movement occurred along a bedding plane. The detachment crown was located along a sub-vertical joint, according to in situ observations. The precipitation data showed that medium-high intensity rain occurred in the area for two days before the landslide. It was assumed that quarrying released the bedding planes and induced tension cracks to propagate, allowing more rainwater to seep in, which

triggered the landslide. An example of a model of rainfall-induced initiation model is presented by Salciarini et al. (2006). A case of a landslide related to prolonged rainfall patterns is studied by Ibsen and Casagli (2004).
The stability analyses were carried out by using the limit equilibrium method (Janbu solution) implemented in SLOPE-W (Geo-Slope International, 1998). A section in the middle of the landslide was considered for the analyses (Figure 10). The model is constituted by a single material, characterized by disturbed rock mass mechanical parameters. The anisotropic function was used to introduce Mohr-Coulomb parameters, obtained by the linearization of the Barton-Bandis criterion, along the sliding surfaces. The parameters listed in Table 4 have been considered.

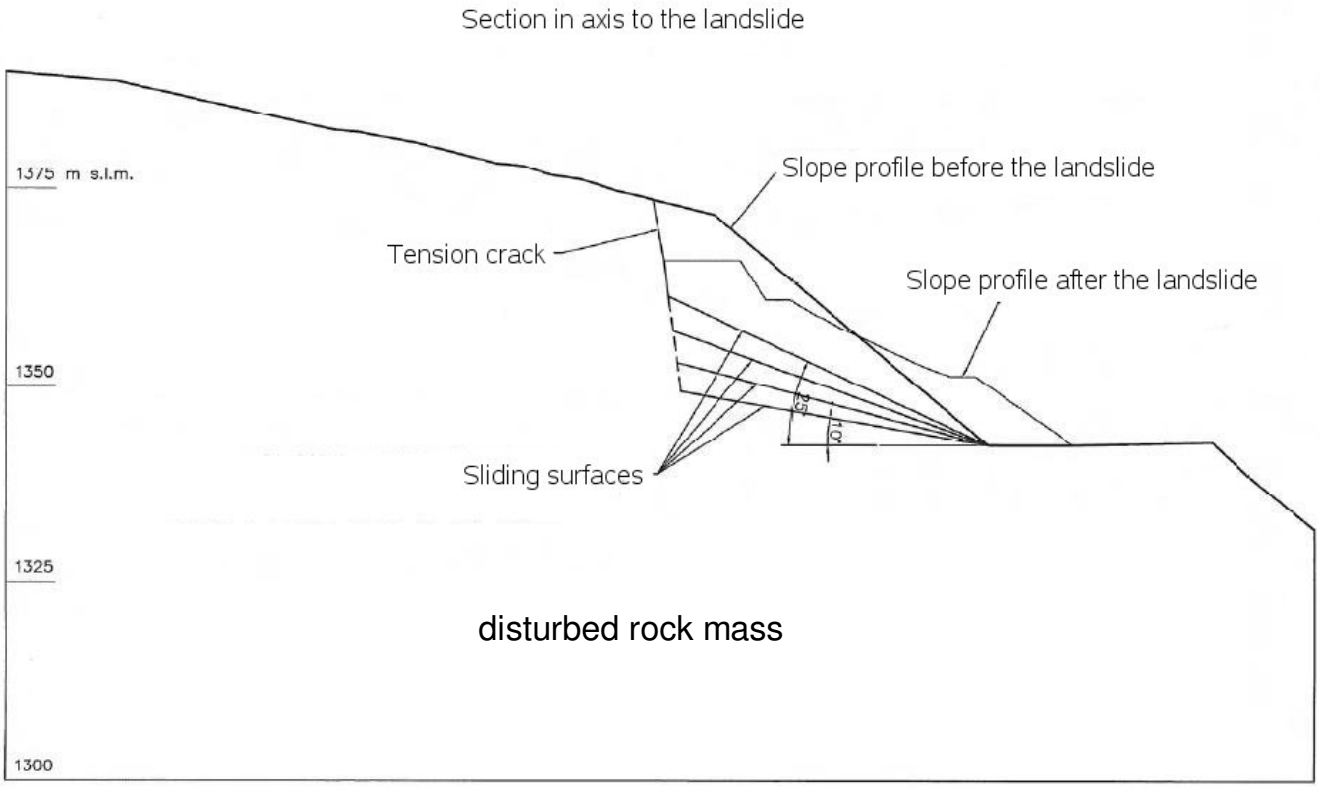

Figure 10. Slope section used for the limit equilibrium analyses (Slope-W).

Table 4. Mechanical parameters ranges used for the back analyses.

Sliding surface cohesion c_j (kPa)	Sliding surface friction φ_j (°)	Dip of the sliding surface (°)	Water in the tension crack (% of crack height) (%)
From 0 to 50	From 26 to 34	From 10 to 25	From 0 to 80

In the cases of 20° to 25° sliding surface dips, limit equilibrium (i.e., safety factor $F = 1$) is reached for a water level in the tension crack of about 40% to 60% of its height and strength parameters very close to that obtained from the geotechnical characterization: 0 kPa/32°, 4 kPa/30° and 9 kPa/28° (cohesion/friction angle). According to the geotechnical characterization results and in situ observations, the last set of parameters was chosen as residual characteristics for the bedding planes.

Slope stability analysis in natural condition

To understand the instability mechanisms in the hill, a number of 2D numerical slope stability analyses were carried on by modeling the slope as an equivalent continuum, with the Finite Difference Method implemented in FLAC code (Fast

Lagrangian Analysis of Continua; ITASCA, 2006). The aim of the simulations was to estimate the global safety factor for the slope by using the SSR method (Shear Strength Reduction), for different hydraulic scenarios.
A section of interest was modeled (section A-A in Figure 1 and Figure 11, left), in the NE-SW direction, between the broadcasting site and the pit, across the zone in which tension cracks were observed and close to the landslide. According to the geotechnical characterization, two materials with different mechanical characteristics were used in the model: one to represent the fractured fault zone in the central part of the model, below the broadcasting plant, and the other to simulate the undamaged rock mass.
Following the inclinometric and stratigraphic evidences, two interfaces were introduced in the upper part of the slope (Figure 12), at about 8 and 16 m from the ground level, to simulate the presence of a more deformable layer. In order to simulate the bedding planes characterized by high persistence and down slope dipping, the rock mass was considered homogeneous and anisotropic, with ubiquitous joints, dipping of 20° and the mechanical properties obtained with the back-analysis (see the previous subsection).
An ideal elasto-plastic model was considered for the rock mass, the interfaces and the ubiquitous joints. Plane strain conditions were assumed in 2D analyses. The strength and deformability parameters used in the numerical analyses, defined by the geotechnical characterization (minimum values), reduced by a partial safety factor of 2 for the cohesion and 1.25 for the friction coefficient, are collected in Table 5. The model was discretized with quadrangular, four-nodes plane elements; the presence of the warehouse on the top of the slope has been simulated using quadrangular elements with linear elastic behavior (unit weight: 10 kN/m^3, elastic parameters equal to those of the undisturbed rock mass). A vertical force of 1000 kN and a horizontal force of 915 kN were applied on the top of the slope, to simulate the broadcasting tower loading, according to the tower design data (Figure 11, right).
The hydraulic scenarios were defined on the base of the only available information: at a depth of about 25 m from the ground level, the presence of water was observed in the rock mass in the pit. In order to analyze the stability of the slope also in the case of water level rising, a 5 m depth water level was considered, i.e., a complete saturation of the rock mass below the surface layer considered as permeable. From there, three scenarios were selected:

- water table at 5 m from the level of site, without the presence of ubiquitous joints,
- water table at 25 m from the level of site and presence of ubiquitous joints,
- water table at 5 m from the level of site and presence of ubiquitous joints.

The analyses results show a global factor of safety varying between 2.1 (scenario 3) and 2.8 (scenario 1), confirming the stability of the slope in the past.
The results also show the development of a shear band parallel to the slope profile, at a depth of about 15-20 m for scenario 3 and 5-10 m for scenario 2. This confirms that the transversal isotropy induced by the bedding planes is a predisposing cause of sliding. The presence of water in the rock mass also reduces the stability of the slope.

Table 5. Mechanical parameters for the numerical analyses (c represents the cohesion, φ the friction angle, E_d the deformability modulus, ν the Poisson ratio, K_n and K_s the normal and tangential stiffness of the discontinuities).

Element	c (kPa)	φ (°)	E_d (MPa)	ν (-)	K_n (MPa)	K_s (MPa)
Undisturbed rock mass	148	54	4500	0.35	-	-
Ubiquitous joints in undisturbed rock mass	10	30	-	-	-	-
Interfaces of undisturbed rock mass	10	30			26808	9930
Fault zone	42	36	400	0.40	-	-
Ubiquitous joints in fault zone	10	28	-	-	-	-
Interfaces in fault zone	10	28	-	-	2090	774

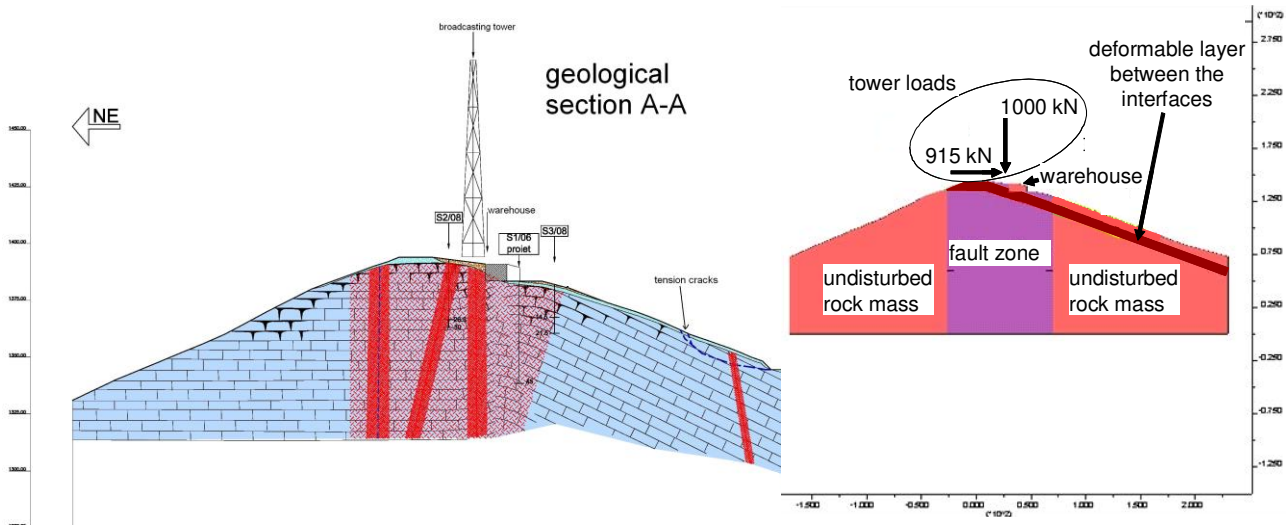

Figure 11. Geological section A-A (left) and model for numerical analyses (right).

Analyses of the slope stability after the landslide

The slope behavior after the landslide in the pit area was simulated. It was assumed that the landslide induced a stress release in the slope beside it, between 1345 m and 1375 m above sea level with down slope displacements. For this purpose, a 20 m thick layer of the rock mass (equal to the estimated depth of the landslide) has been relieved between 1345 m and 1375 m above sea level. In order to simulate the progressive failure along the critical layer, the deformability and strength properties of the corresponding elements were progressively reduced (Table 6 and Figure 12).
The results show an important displacement increase in the upper part of the slope. The displacements in the warehouse area are appreciable only in the case of water table at 5 m from the level of site (Figure 13). A wide area in the disturbed rock mass reaches the plastic boundary for every hydraulic scenarios. From this, it is possible to reconstruct the slope's stress-strain history. The cuts in the pit area induced a progressive instability in the area immediately below the broadcasting plant, with downwards displacements that started in the pit cut and spread towards the warehouse. The landslide in the pit area quickened the instability phenomenon that worsened with heavy rain falls, leading to considerable displacements in the warehouse area.

Table 6. Mechanical parameters for the numerical analyses (layer between 8 and 16 m).

Element	c (kPa)	φ (°)	E_d (MPa)	ν (-)	K_n (MPa)	K_s (MPa)
Undisturbed rock mass	148	54	2250	0.35	-	-
Ubiquitous joints in undisturbed rock mass	0	30	-	-	-	-
Fault zone	42	36	200	0.40	-	-
Ubiquitous joints in fault zone	0	28	-	-	-	-
Interfaces in fault zone	0	28	-	-	1022	741

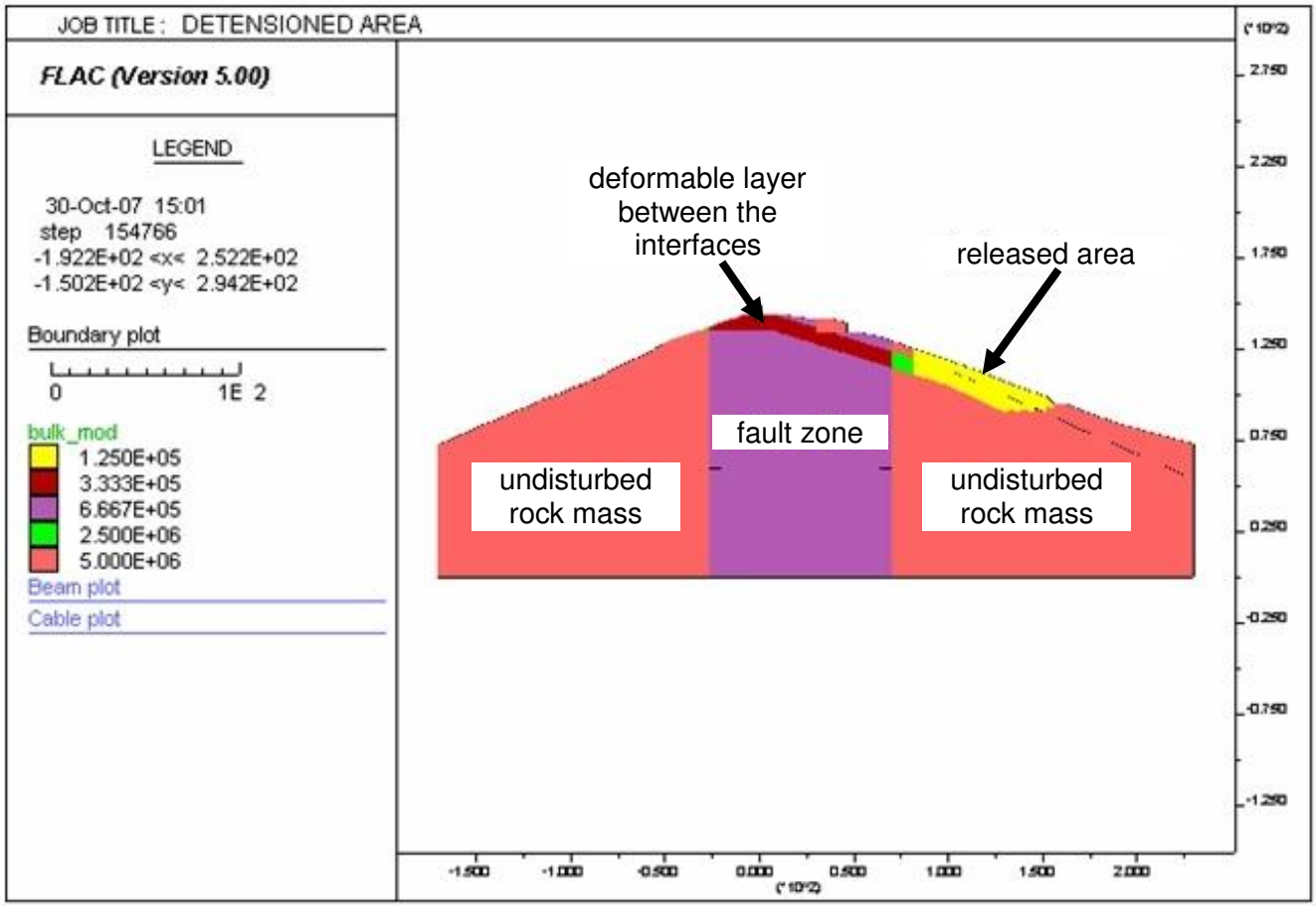

Figure 12. Model with released area to simulate the landslide in the pit (FLAC).

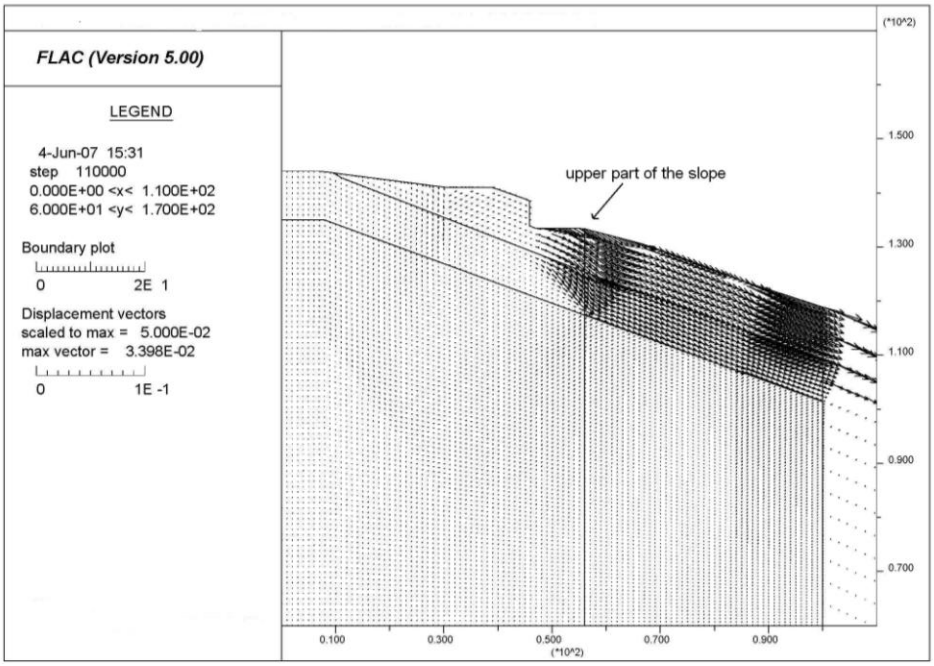

Figure 13. Numerical results: displacements in the upper part of the slope.

Effects of the mining activity progression on the slope stability

In order to understand the effects on the broadcasting plant stability of the progression of the mining activity toward it, additional numerical analyses were carried out on the same model considered for the previous analyses. The progressive excavation of the pit until it reached section A-A, in the horizontal direction with a 45° face dip was simulated (Figure 14), progressively removing the mesh elements belonging to the excavation area.
The obtained results pointed out that, with the extension of the pit area, the displacements in the upper part of the slope increase. Close to the warehouse they become in the order of a few centimeters. In particular, the displacements become considerable when the excavation involves the deformable layer.
The results allow to assert that a progression of the mining activity toward the broadcasting plant would induce its instability. For this reason, it can be considered as a triggering cause of the slope movement. As such, it should not to be authorized.

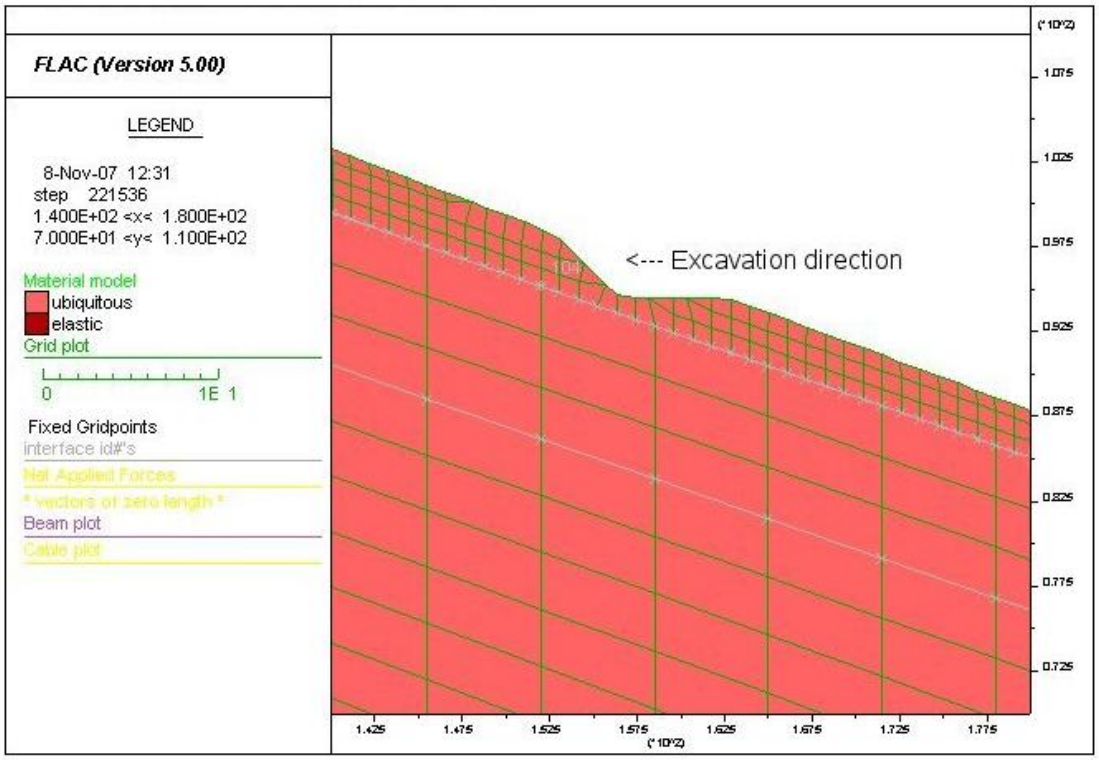

Figure 14. Model for the progression of the mining activities analysis.

SLOPE STABILIZATION MEASURES

The analyses highlight the precarious condition of the broadcasting installation and the need to actively enhance its stability. For this purpose, the first essential action is to stop the quarry from encroaching closer to the tower area. To reduce and limit the hydraulic pressure into the slope, the following measures have to be taken:

1. sealing the cracks with mortar or resins at the top of the slope to reduce infiltration of water ;
2. turfing of the critical area of the slope, between 1345 m and 1375 m;
3. installation of sub-horizontal drains (microfissured PVC pipes), starting from the foot of the landslide in the pit area, so that residual water inside the slope is drained;
4. interception of runoff in the southern area of the site and channeling it to the slope at the back of the plant, where there is no apparent instability problem;
5. continuous monitoring by inclinometer and crack gauges in the warehouse area.

In order to confine the strain effects of the stress release induced by the landslide, the broadcasting site has to be isolated from the unstable slope. For this purpose, a structural stabilization system in the warehouse square was suggested (Figure

15 and 17). It was conceived to be a bulkhead consisting of 27 m long micropiles reinforced with steel pipes, 139.7 mm of diameter and 10 mm thick. The micropiles are connected at their head level by a reinforced concrete beam. The bulkhead extends as shown in Figure 15 and is anchored in the head to the undamaged rock mass by means of 28 m long four strands steel anchors, at center distance of 3 m and with a down dipping of 25°. During the construction of the bulkhead, any karst cavities will be filled.

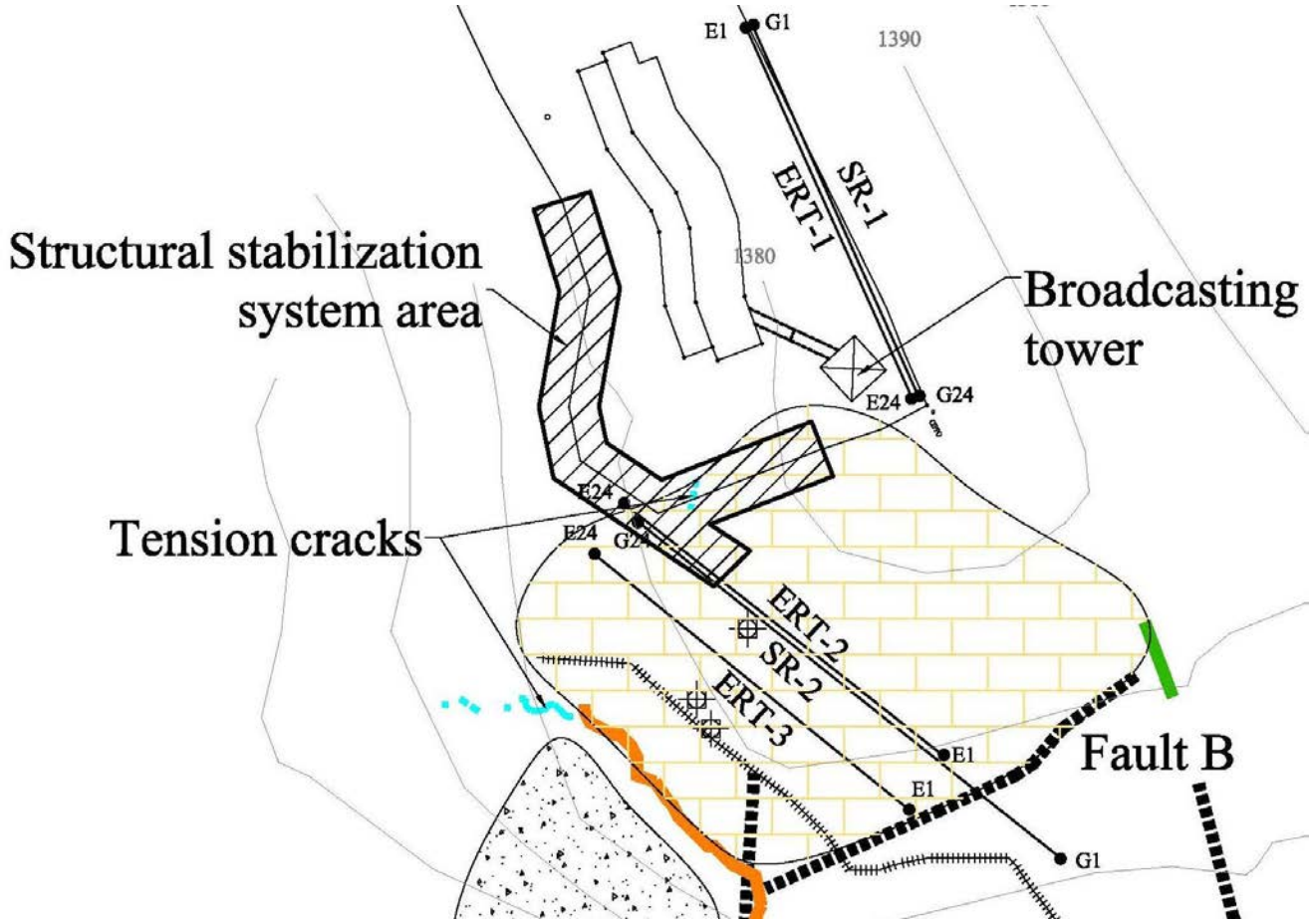

Figure 15. Map of the site with the location of the stabilization system.

Numerical verification of the stabilization system

To verify the length of the micropiles, numerical analyses were carried out assuming different length of the bulkhead micropiles (from 6 m until 35 m). The same model used for the analyses without support was considered, in which the support system was introduced with beam elements for the micropiles and cable elements for the anchors. The worst hydraulic scenario was considered with the water level at a depth of 5 m from the level of site.

The results (Figure 16) confirm that the minimum length for the micropiles is about 16 m (the depth at which the boundary between the weaker layer and the undisturbed rock mass is located). On the other hand micropile lengths greater than 20 m don't provide further benefit to the plant stability. It is possible to conclude that 27 m is a good estimate of the length for the micropiles.

To confirm the global effectiveness of the suggested structural stabilization system, four monitoring points were selected in the model close to the warehouse, upstream and downstream with respect to the bulkhead and into the landslide in the pit area. The displacements obtained from numerical analyses with and without the support are shown in Table 7. It can be observed that the structural support system allows to significantly reduce the displacements in the plant area. Moreover the

numerical analyses provided the normal force, bending moment and shear force acting on the micropiles and the axial forces acting on the anchors (Figures 17, 18 and 19). These results were used to design the steel elements.
LEM analyses were carried out on the same section, with and without the structural stabilizing elements. An increase of the global factor of safety of about 0.25 was obtained if the support is present (global factors equal to 2.6 and 2.85 were calculated without and with support, respectively). Further analyses in which the progression of the mining activity was simulated in the model with support were carried on. The results showed that, in spite of the presence of the stabilization system, the displacements in the plant area are unacceptable. This confirms that the interruption of the mining activity is the first safety measure to take.

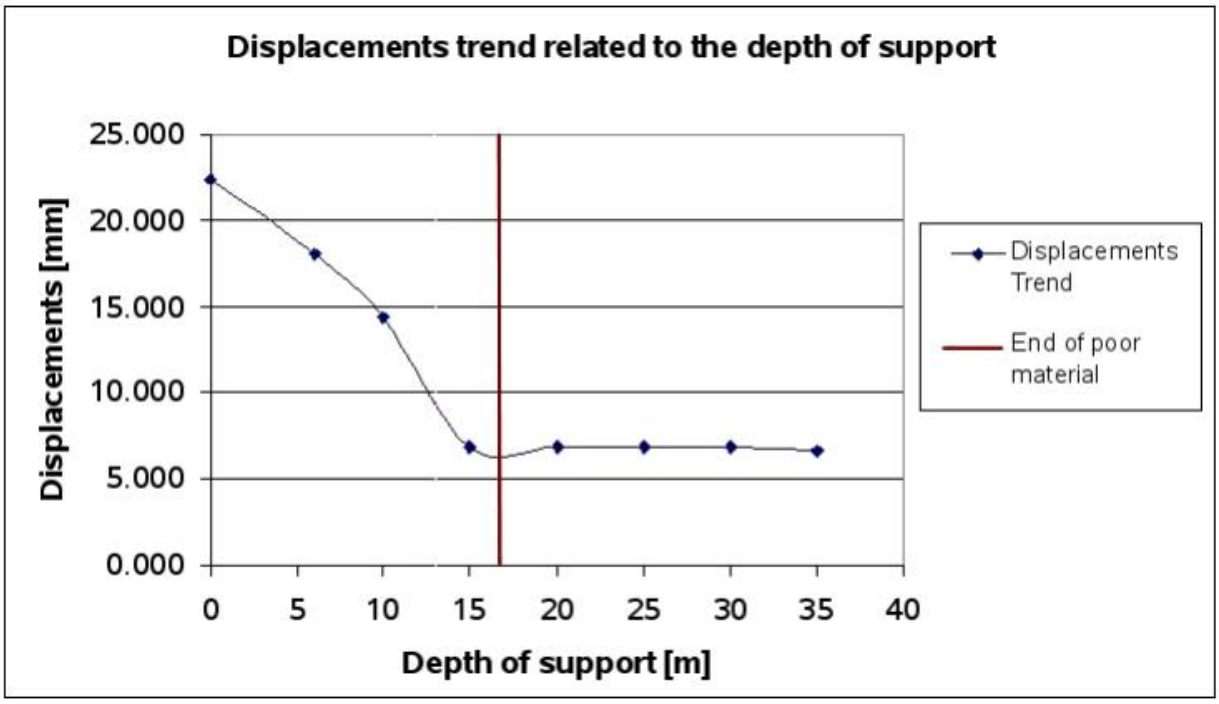

Figure 16. Model displacements in the area upstream the bulkhead, related to the length of the micropiles (assuming that in-situ bedrock is at 16 m depth).

Table 7. Displacements values with and without the support.

Analysis	Displacements in the landslide (mm)	Displacements downstream the bulkhead (mm)	Displacements upstream the bulkhead (mm)
Without support	57.0	35.5	22.4
With support	56.0	35.8	6.9

FURTHER DEVELOPMENTS

Upon completion of the study, on the basis of the monitoring measures, some further observations have been formulated:

- the broadcasting tower is not affected by the landslide. The stabilizing system, isolates the tower and warehouse area ensuring the tower safety,
- the mining activity toward the broadcasting has stopped, as suggested.

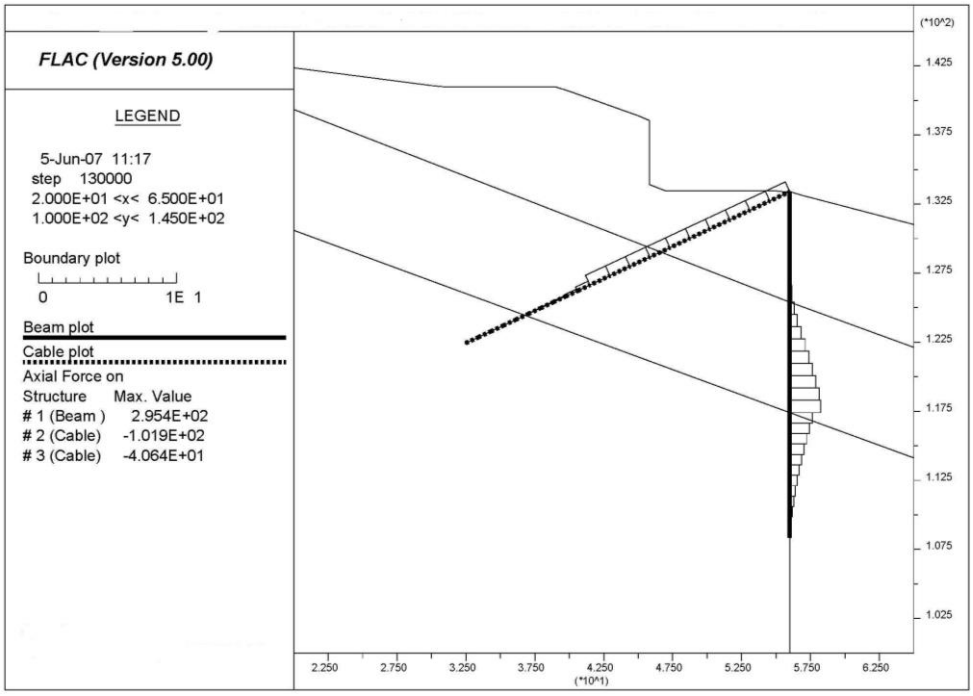

Figure 17. Axial forces acting on micropiles and anchors.

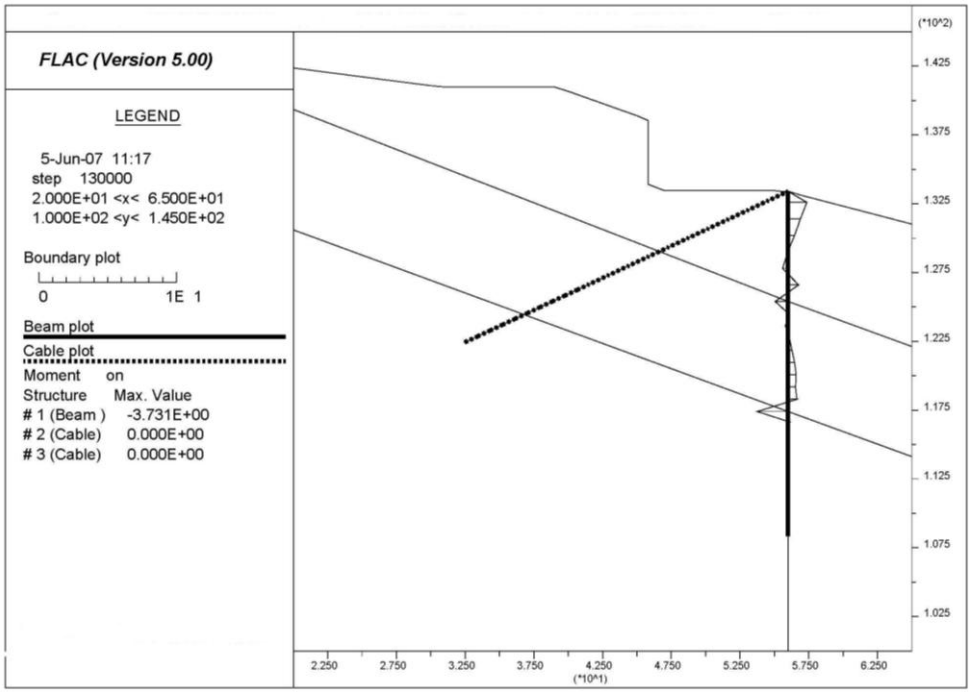

Figure 18. Bending moment acting on micropiles.

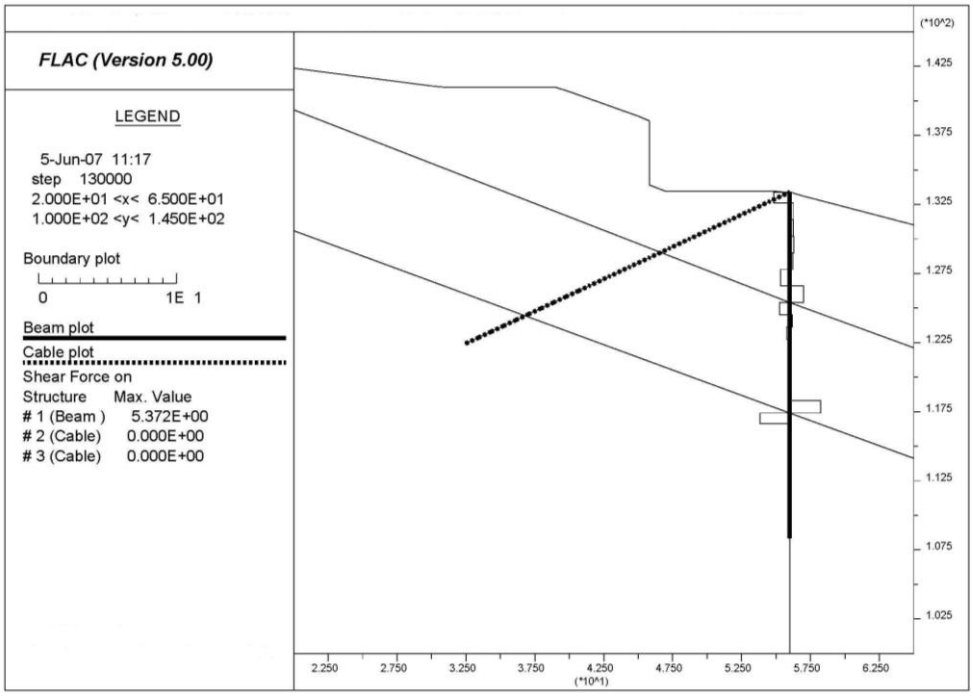

Figure 19. Shear force acting on micropiles.

CONCLUSIONS

In order to investigate the stability conditions of the broadcasting plant, an extensive geological, geotechnical and geophysical survey and detailed numerical simulations have been carried out. An inclinometer has been installed in the warehouse area and the main cracks in the warehouse have been instrumented with crack gauges. The core drilling analysis and the geological and geomorphological data allowed the identification of the following main causes of instability:

1. complex structural and geological rock mass conditions: the rock mass is characterized by two main fault systems, a set of bedding planes, and two sets of sub vertical discontinuities, that can be potential tension cracks,
2. meteoric water infiltration in the rock mass fractures, with the onset of appreciable hydraulic pressures,
3. mining activity at the base of the slope towards the plant area, that excavate the slope releasing the bedding planes.

As no damages occurred in the buildings located in the broadcasting site neighborhood and no movements occurred in the broadcasting tower, it was possible to assert that the instability phenomenon was not induced by a larger deep seated landslide.

Following these observations, a number of numerical analyses have been carried out with the main goal of suggesting safety measures to provide the overall stability of the broadcasting plant. The authors suggested the following activities:

- rain fall water collection in the stable part of the slope,
- drain system to reduce deep water infiltration in the rock mass,
- bulkhead in the warehouse square to confine the broadcasting plant from the instable slope,
- interruption of the progression of the mining activity toward the broadcasting plant,
- monitoring of the slope during the bulkhead construction and thereafter for adequate time to confirm the effectiveness of the countermeasures suggested.

ACKNOWLEDGMENTS

The Authors wish to acknowledge Domenico Parisi of GEODES Srl, Turin, for his invaluable support.

REFERENCES

Barpi F., De Giorgio L. and Grandi S. (2008). "Instability of a broadcasting plant induced by a landslide." Proceedings of the Fourth International Forensic Engineering Conference, London, 2-4 December 2008, 315-324.

Bandis S.C. (1993). "Engineering properties and characterization of rock discontinuities." In Comprehensive Rock Engineering, Pergamon Press, London, 1 (6), 155-183.

Eberhardt E. (2003). "Rock slope stability analysis – Utilization of advanced numerical techniques." Vancouver, Canada: Earth and Sciences, UBC, 17-81.

Ferrero A.M. and Segalini A. (2011). "Assessment of stability conditions of ancient underground quarries using on-site monitoring and numerical modeling." International Journal of Geoengineering Case Histories, 1 (2), 66-85.

Geo-Slope International Ltd. (1998). "SLOPE-W v. 4" Calgary, Alberta (Canada)

Hampson D. and Russel B. (1984). "First break interpretation using generalized linear inversion." Journal of the Canadian Society of Exploration Geophysicists, 25, 40-50.

Hoek E. and Brown E.T. (1980). "Empirical strength criterion for rock masses." Journal Geotechnical Engineering Division (ASCE),106, 1013-1025.

Hoek E. and Brown E.T. (1997). "Practical estimates of rock mass strength." International. Journal of Rock Mechanics & Mining Science & Geomechanics Abstracts. 34 (8), 1165-1186.

Hoek E., Carranza Torres C. and Corkum B. (2002). "Hoek-Brown failure criterion – 2002 edition." Proceedings of the North American Rock Mechanics Society Meeting, Toronto, 267-273.

Hoek E. and Diederichs M.S. (2006). "Empirical estimation of rock mass modulus." International Journal of Rock Mechanics and Mining Sciences, 7, 81 43, 203-215.

Ibsen M.L. and Casagli N. (2004). "Rainfall patterns and related landslide incidence in the Porretta-Vergato region, Italy." Landslides, 1(2), 143-150.

Olsen K.B. (1989). "A stable and flexible procedure for the inverse modeling of seismic first arrivals." Geophysical Prospections, 37, 455-465.

Pelizza S., Oreste P.P., Peila D. and Oggeri C. (2000). "Stability analysis of a large cavern in Italy for quarrying exploitation of a pink marble." Tunnelling and Underground Space Technology, 15(4), 421-435.

Salciarini D., Godt J.W., Savage W.Z., Conversini P., Baum R.L. and Michael J.A. (2006). "Modeling regional initiation of rainfall-induced shallow landslides in the eastern Umbria Region of central Italy." Landslides, 3 (3), 181-194.

ITASCA Consulting Group (2006). "FLAC (Fast Lagrangian Analysis of Continua), User Manual" Minneapolis (USA).

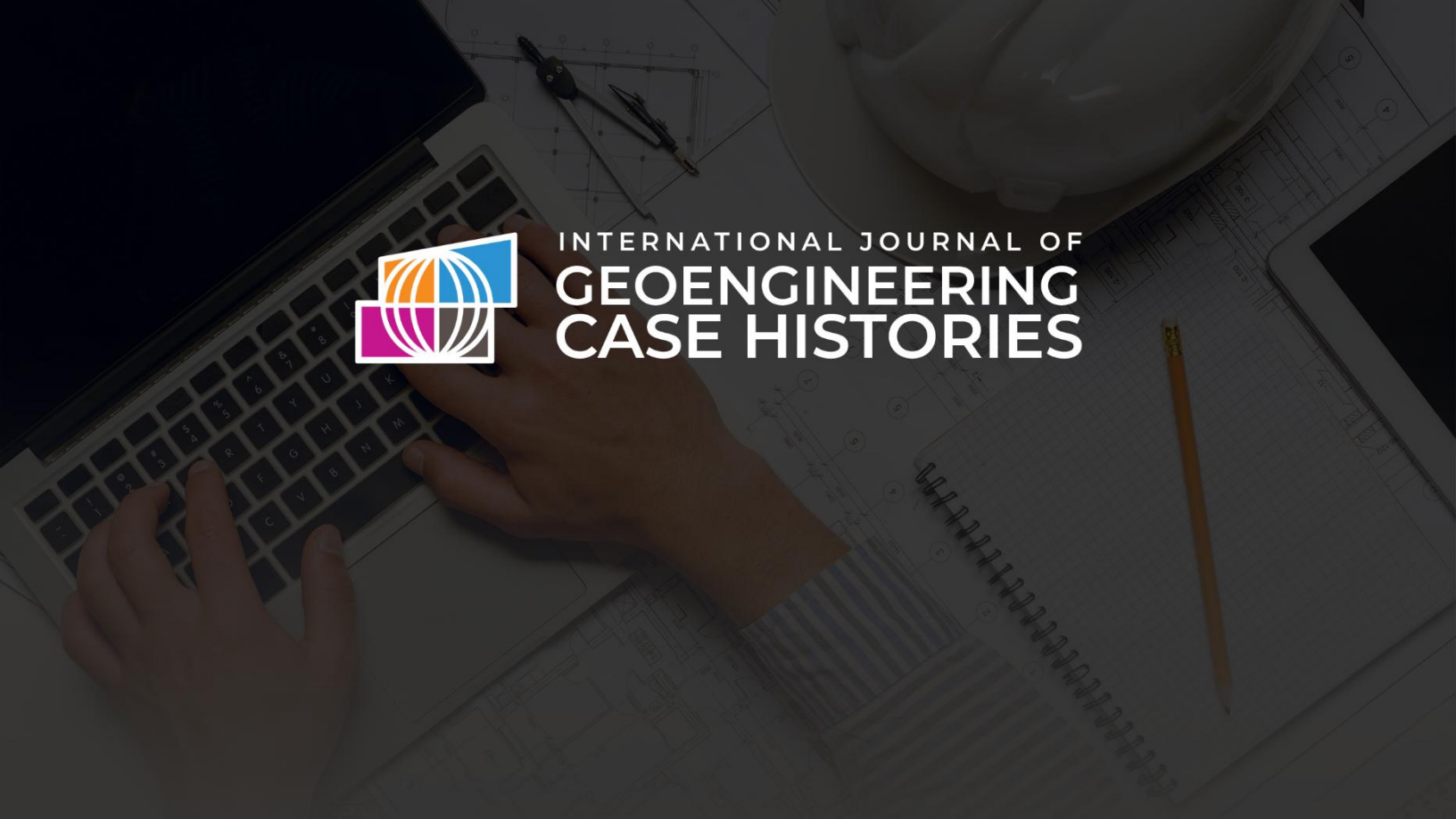

INTERNATIONAL JOURNAL OF
GEOENGINEERING
CASE HISTORIES

The Journal's Open Access Mission is generously supported by the following Organizations: